NUMERIC SIMULATIONS FOR SENSING THROUGH THE WALL RADAR

Traian Dogaru* and Calvin Le
U. S. Army Research Laboratory
Sensors and Electron Devices Directorate
Adelphi, Maryland 20783-1197

ABSTRACT

This paper presents numeric simulations related to sensing through the wall radar technologies. Our computational approaches include the Finite Difference Time Domain (FDTD) algorithm and the shooting and bouncing ray technique (Xpatch). We analyze the radar signatures of the human body and other objects, in free-space and inside a room. The emphasis is on radar scattering phenomenology, with results presented as Radar Cross Section (RCS) and Synthetic Aperture Radar (SAR) images.

1. INTRODUCTION

Sensing Through The Wall (STTW) has emerged as a key radar application during the last few years, as part of the Sensors and Communications (C4ISR) Vision requirement for the Future Force Warrior. The interest in this technology is reflected by the fact that several major programs related to STTW radar are currently funded by all three branches of the military and DARPA. At the Army Research Laboratory (ARL), we are drawing on almost two decades of experience in radar detection and imaging of targets in concealed environments, such as foliage penetrating radar (FOPEN) and ground penetrating radar (GPR) (Ressler et al., 1995, Carin et al. 1999). The common challenge for these scenarios is finding a balance in minimizing the electromagnetic propagation loss while maintaining a realistic antenna size/power requirement. Operating the radar in the low frequency microwave range (300 MHz to 3 GHz) has the advantage of good penetration through building structures. At the same time, Ultra-Wideband (UWB) excitation and Synthetic Aperture Radar (SAR) technologies are employed in order to obtain good image resolution. Our simulations of STTW radar allow us to predict the Radar Cross Section (RCS) of targets of interest (such as the human body) and generate SAR images of complex scenes (such as a room with objects inside). Based on our models, we are able to make recommendations to radar system designers with regard to essential parameters, such as frequency of operation, bandwidth, aperture size, polarization etc. In this paper, we demonstrate our capabilities in simulating complex STTW radar scenarios and draw some important conclusions regarding such radar system design and operation.

2. COMPUTATIONAL APPROACHES

There are several problems of interest in simulating STTW radar scenarios and understanding the underlying phenomenology. One is studying the radar signature of the human body and its variation with frequency, aspect angle, position of the human etc. At a larger scale, we are interested in the radar imagery of full rooms or building structures, including humans and other objects inside. In terms of modeling tools, we are leveraging the hardware and software infrastructure available to us at the Army Research Laboratory, consisting of a suite of electromagnetic codes for radar signature computation, as well as the massive parallel computer systems at the Army Major Shared Resource Center (MSRC).

During the 1990's, concerns about the health effects of electromagnetic radiation within the wireless industry prompted a number of studies on the propagation of electromagnetic waves in the presence of a human body (Lazzi et al., 1998, Tinniswood et al., 1998, Toftgard et al., 1993). The Finite Difference Time Domain (FDTD) method (Taflove, 1998) was the natural candidate to modeling this type of problems, given the complexity of human tissues dielectric properties. However, most of these studies were oriented towards computing the radiation absorption rates inside the human body. The recent focus on military and national security applications and the emergence of the Ultra-Wideband (UWB) microwave radar as a promising technology for detecting the human presence in concealed environments, calls for employing the FDTD algorithm in analyzing the radar response of the human body. Such models are very useful in designing and predicting the performance of the radar system.

We started with the human body model available on the web at the US Air Force Research Laboratory, RF Radiation Branch site. This site stores highly

Report Documentation Page

Form Approved
OMB No. 0704-0188

1. REPORT DATE	2. REPORT TYPE	3. DATES COVERED
01 NOV 2006	**N/A**	**-**

4. TITLE AND SUBTITLE	5a. CONTRACT NUMBER
Numeric Simulations For Sensing Through The Wall Radar	5b. GRANT NUMBER
	5c. PROGRAM ELEMENT NUMBER
6. AUTHOR(S)	5d. PROJECT NUMBER
	5e. TASK NUMBER
	5f. WORK UNIT NUMBER
7. PERFORMING ORGANIZATION NAME(S) AND ADDRESS(ES) **U. S. Army Research Laboratory Sensors and Electron Devices Directorate Adelphi, Maryland 20783-1197**	8. PERFORMING ORGANIZATION REPORT NUMBER
9. SPONSORING/MONITORING AGENCY NAME(S) AND ADDRESS(ES)	10. SPONSOR/MONITOR'S ACRONYM(S)
	11. SPONSOR/MONITOR'S REPORT NUMBER(S)

12. DISTRIBUTION/AVAILABILITY STATEMENT
Approved for public release, distribution unlimited

13. SUPPLEMENTARY NOTES
See also ADM002075., The original document contains color images.

14. ABSTRACT

15. SUBJECT TERMS

16. SECURITY CLASSIFICATION OF:			17. LIMITATION OF ABSTRACT	18. NUMBER OF PAGES	19a. NAME OF RESPONSIBLE PERSON
a. REPORT	b. ABSTRACT	c. THIS PAGE			
unclassified	**unclassified**	**unclassified**	**UU**	**8**	

detailed FDTD-compatible grids, where the dielectric properties of each human tissues are sampled using 1 mm, 2 mm or 3 mm cubic cells. The complex permittivities of tissues are given as parametric functions of frequency. However, our FDTD code handles only materials with constant (real part-) permittivity and conductivity over frequency, so we had to compute these values at the central frequency of our simulations. The effect of this approximation on the human body RCS will be discussed later. We also employed the Varipose software to articulate the body into various positions. The purpose is to investigate the variability of human signatures in order to develop automatic target detection algorithms. Since this requires careful consideration to modeling details, we used the three-dimensional Finite-Difference Time-Domain (FDTD) code developed at the Army Research Laboratory. This is an exact electromagnetic solver that can handle almost arbitrary shapes and media configurations. Our code is fully scalable, designed to run on several High Performance Computing (HPC) platforms.

Although FDTD would also enable us to obtain exact radar scattering models for entire rooms, this technique is very computational intensive. For example, modeling a 5 m x 4 m x 2.2 m room by this method requires on the order of 24 GBytes of RAM and 144 CPU hours, to obtain the signature at one angle. On the other hand, approximate solvers, such as Xpatch (a ray tracing code combining geometrical and physical optics), can provide reasonably accurate results in considerably less time (on the order of 1000 times faster) (Andersh et al., 1994, Andersh et al., 1998, Andersh et al., 2000). An important part of our work was on validating the Xpatch results against an exact solver (FDTD), for scenarios of interest in STTW. Our comparison between Xpatch and FDTD showed remarkable agreement in most situations, with deviations usually not exceeding 2 dB. This enabled us to confidently apply Xpatch to simulating radar imaging for a number of complex scenarios, involving full size rooms, equipped with interior dividing walls, furniture, humans, weapons etc.

3. RESULTS

3.1. FDTD modeling of the human body

Fig. 1 represents the three-dimensional FDTD grid for the standing human (basic position). For the 3 mm grid, the computational domain size was 236 x 154 x 666 cells. We also performed simulations on the 2 mm grid, for which the computational domain size was 333 x 210 x 979 cells. In Fig. 2 we show the FDTD grid for a kneeling human (the new position was obtained with Varipose). In this case, the 3 mm resolution computational domain was 233 x 495 x 612 cells. Since we are interested in RCS-type calculations, the sources and receivers are assumed in the far field. The depression angle is always zero degrees (**k** vector in the *x-y* plane), the human is placed in free-space and we always consider a monostatic radar configuration. The excitation pulse is Rayleigh 4th order, with a central frequency of either 1 GHz or 3 GHz, which is representative for UWB microwave radar. Its 3 dB band extends from about $0.5f_c$ to $2f_c$ (where f_c is the central frequency).

We considered front (broadside) incidence for the basic standing position in Fig. 3, both V-V and H-H polarizations, with 1 GHz central frequency excitation and the 3 mm grid. As one can notice, the two polarizations yield very similar RCS. One important question is whether the 3 mm cell size is fine enough to accurately represent the electromagnetic wave propagation through the human body. At 1 GHz and 3 mm cell size, the spatial sampling rate is 100 in free-space. However, some tissues in the human body have very high relative permittivity (in the 40-60 range), which makes the effective sampling rate within those media much smaller than in free-space. In order to assess the frequency limit where the RCS results on the 3 mm grid become inaccurate, we ran the same simulations on a 2 mm grid, over the 0-9 GHz band. The results, shown in Fig. 4 (V-V polarization only), indicate that the match is reasonably good up to 5 GHz, but the 3 mm grid may be inadequate for simulations above this frequency.

Another question we tried to answer was how much the penetration of electromagnetic radiation through the human body had an influence on the RCS. In Fig. 5 we compared the RCS of the 'real' model to that of a man made of a uniform material with dielectric properties close to the skin (V-V polarization). At $\varepsilon_r = 50$, $\sigma = 1$ S/m, this material acts almost as a perfect reflector, so penetration in this case should not play a significant role in the RCS. Looking at the two graphs, we concluded that, except for low frequencies (up to 1.2 GHz), the penetration through the body is not important in RCS calculations. However, as expected, the lower frequencies do penetrate the thin layer of skin and hit a relatively low dielectric/loss fat tissue, bouncing back and creating interference.

With regard to the constant permittivity/conductivity limitation of the FDTD code, we ran a simple test to evaluate its impact on our models.

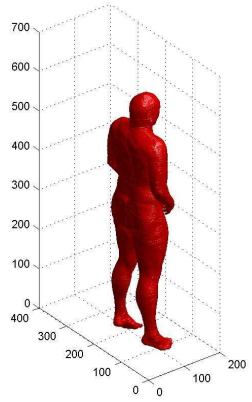

Fig. 1. Three-dimensional FDTD grid for the human in the basic standing position.

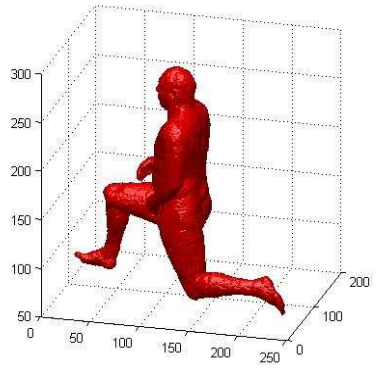

Fig. 2. Three-dimensional FDTD grid for the human in the kneeling position.

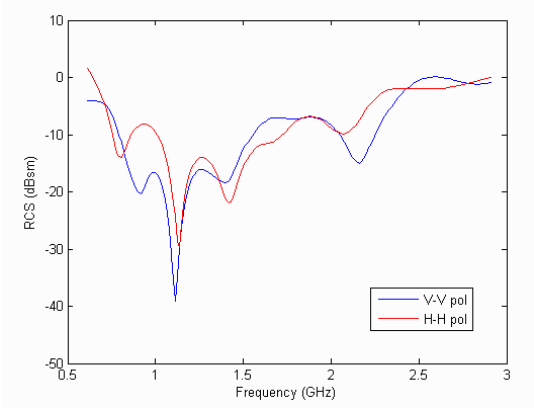

Fig. 3. RCS of the human body in the basic standing position, front (broadside) incidence, 3 mm grid.

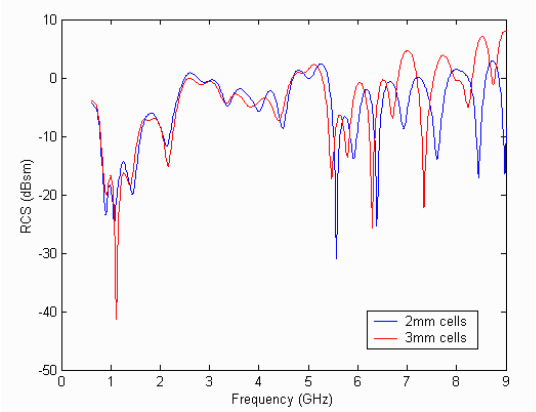

Fig. 4. RCS of the human body, front (broadside) incidence. Comparison between 2 and 3 mm grid models.

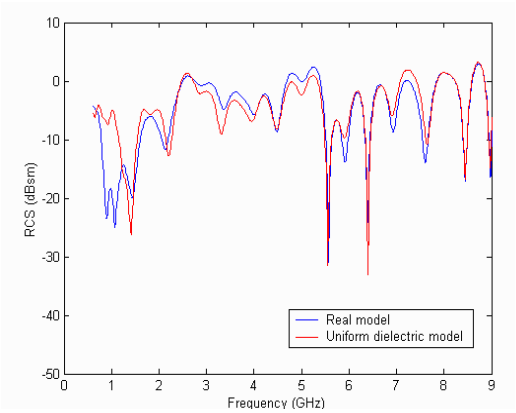

Fig. 5. RCS of the human body, front (broadside) incidence. Comparison between the real model and a uniform dielectric model.

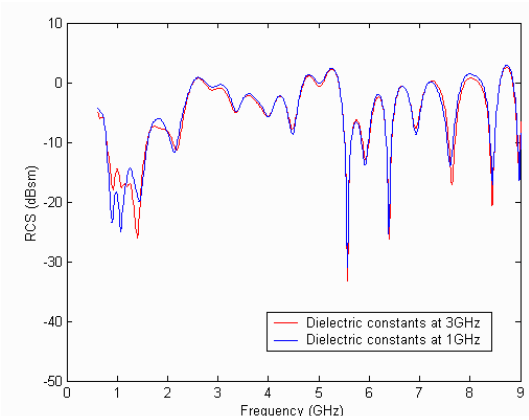

Fig. 6. RCS of the human body, front (broadside) incidence. The effect of frequency-dependent permittivities on the RCS.

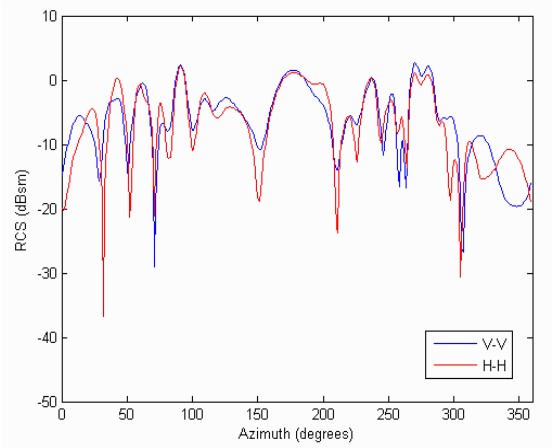

Fig. 7. RCS of the kneeling human as a function of angle, at 1 GHz.

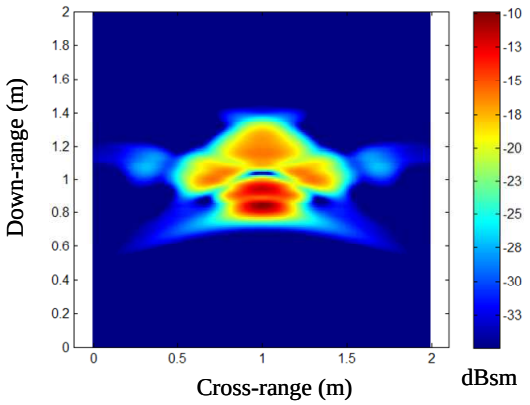

Fig. 8. SAR image of a human body in the basic standing position, top view.

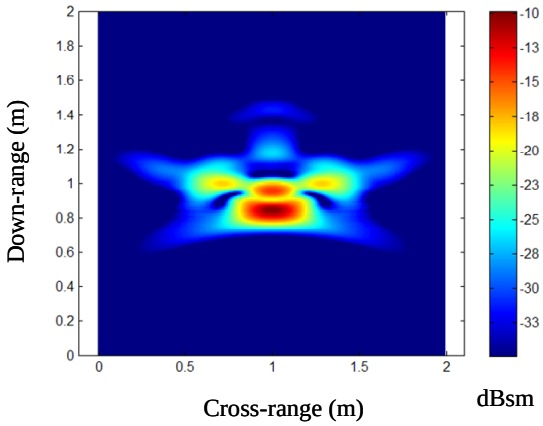

Fig. 9. SAR image of a human body with the legs removed, top view.

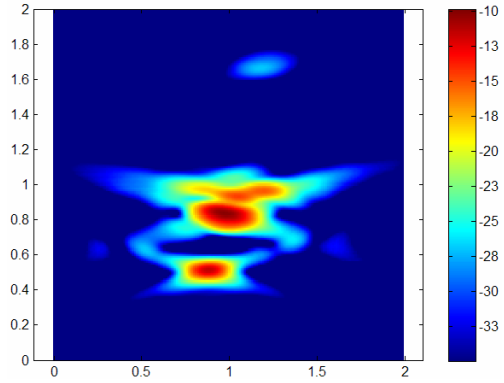

Fig. 10. SAR image of a kneeling human, top view.

First, we utilized the permittivity and conductivity computed at 1 GHz (from the original data), then we ran the same simulation again with the material properties computed at 3 GHz. The results are shown in Fig. 6 and clearly prove that, except around 1 GHz, there is no difference between the two calculations. This is consistent with the previous paragraph conclusion, since the reflection coefficient of the skin is not expected to vary much with frequency. However, the differences around 1 GHz (where we have some penetration through the body) suggest that using constant ε and σ, computed at 1 GHz, is acceptable over a wide band of frequencies.

For the human in the kneeling position, we show the RCS variation with the azimuth angle, at 1 GHz, in Fig. 7. Incidence at 180^0 corresponds to a view from the back, and we notice both a relatively large RCS and slow variation with the angle in this azimuth range. However, at angles corresponding to side views, the variation is much faster – the RCS may swing 10-20 dB within less than 10^0 of displacement. The effect is even more evident at higher frequency. This underscores the difficulty of implementing an automatic target recognition approach to through the wall detection of stationary humans, especially when one considers the complexity of all possible postures.

SAR images can offer more insight with regard to the scattering phenomenology than simple RCS plots. In order to build these images, we used the time-domain FDTD-computed signatures at different azimuth angles. We employed the backprojection algorithm (Soumekh, 1999), with an integration angle of 40^0. At 1 GHz central frequency, the approximate resolution is 10 cm in down-range and 10 cm in cross-range.

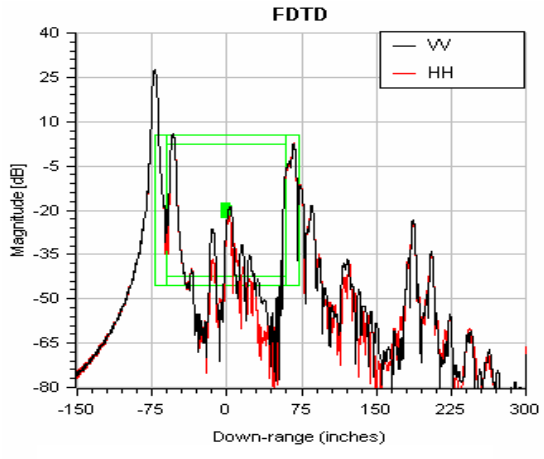

Fig. 11. Range profile for the human in the room obtained with FDTD.

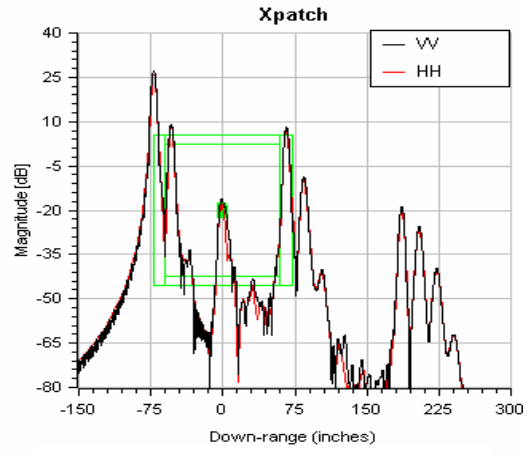

Fig. 12. Range profile for the human in the room obtained with Xpatch.

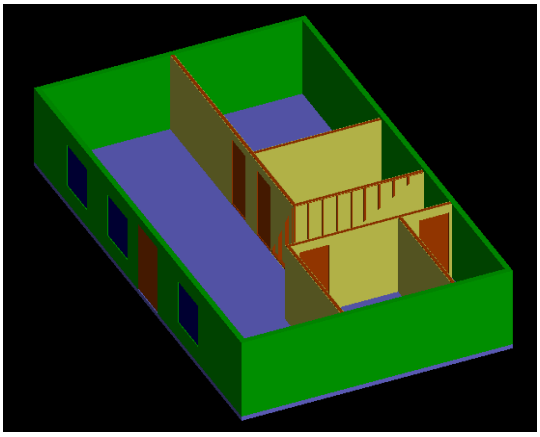

Fig. 13. Building layout for Xpatch modeling (building mapping example).

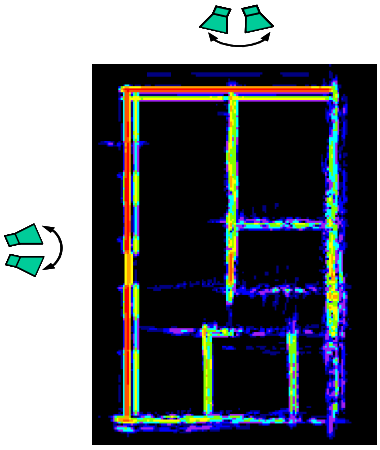

Fig. 14. SAR image of the building in Fig. 13 based on adding the images obtained with two orthogonal apertures.

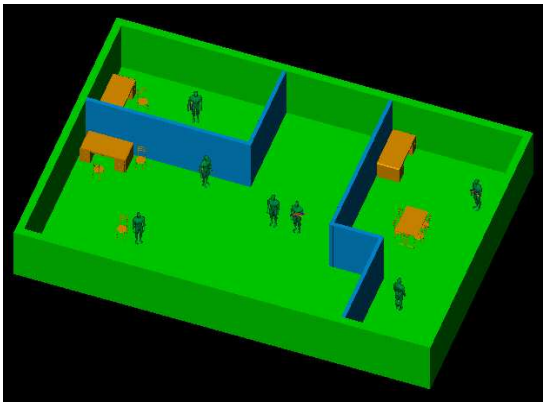

Fig. 15. Building layout for Xpatch modeling (humans in a room example).

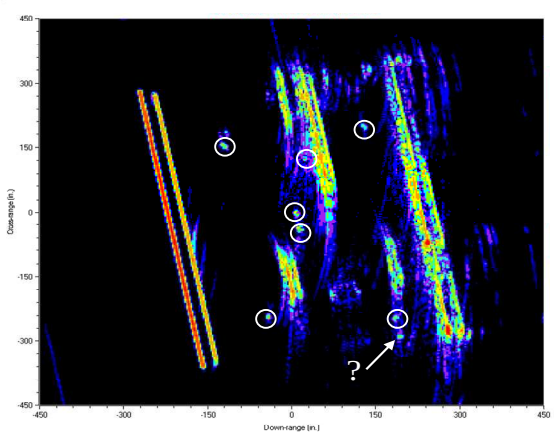

Fig. 16. SAR image of the building in Fig. 15, showing the location of the humans.

In Fig. 8 we depict the image obtained using a 1-GHz-centered pulse and 40^0 integration angle (H-H polarization). This represents a top view (with the man facing down the page) and the intensity scale in dB. One can notice the main scattering center (dark red) in the middle of the image, corresponding to the abdomen and chest of the human. The late-time feature visible in the image appears to be produced by complex wave interactions (surface waves and multiple bounces) with the human legs. To demonstrate that the legs are largely responsible for the late-time feature, we removed them from the body mesh and re-ran the simulation. This operation eliminated most of the late-time response, as shown in the image in Fig. 9. In Fig. 10 we show the SAR image of the kneeling human, with the same radar parameters as above, but in V-V polarization. The right leg appears as a bright scatterer in front of the body, and we also see a trace of the left foot behind the body.

3.2. FDTD vs. Xpatch comparison

As we mentioned above, running an exact electromagnetic model of an entire room in this frequency range is a very computationally intensive task. Our approach was to employ an approximate solver (Xpatch), which utilizes the shooting and bouncing ray technique together with physical optics, in order to obtain a fast solution with reasonable accuracy. Although Xpatch is a mature code that has been successfully used in modeling a variety of radar scenarios at high frequencies (usually X-band or higher), the code has not been applied yet to lower frequencies, between 1 and 3 GHz. In consequence, we first worked on validating the Xpatch results against an exact solver (FDTD) in this frequency range. The scenario we chose for this purpose is a human standing in the middle of a room. The room dimensions are 5 m x 3.5 m x 2.2 m, and the walls are 12" thick, made of brick (ε_r = 2.3-j0.3). We looked at the backscattering response at broadside incidence, perpendicular to the larger (5 m) side wall (the radar is facing the front of the human). The floor and ceiling were taken out in this simulation. The FDTD grid was made of 771 x 1015 x 497 cells and the simulation was run on 24 processors. The center frequency of the excitation was 2.5 GHz, with a bandwidth of 4 GHz.

We present the results as range profiles, in a dB scale, in Figures 11 and 12. The actual room is overlaid in green color in these figures (notice the human appearing as a spot in the middle). The major scattering centers are the front and back sides of the front and back walls, the human, as well as reverberations between the walls which show up in the late time. The amplitudes of return from these main scattering centers are almost the same for both simulation methods. At the same time, we notice that the FDTD range profile has more structure due to secondary scattering effects (multiple diffraction, surface waves, etc.), which are not taken into account by Xpatch. Of particular concern is the third major peak in the FDTD range profile (just before the return from the human), which is probably a multiple edge diffraction effect and does not appear in the Xpatch range profile. However, these secondary effects have relatively low amplitude (under the -30 dB mark in Fig. 11), so they would not play a significant role in a target detection scheme, especially in a noise/clutter environment. We concluded that, despite the limitations inherent to the underlying modeling technique, the Xpatch results are reasonably accurate in problems relevant to STTW radar, and we may confidently apply this code to more complex scenarios.

3.3. Xpatch modeling of complex building structures

Building or room mapping represents one major application of STTW radar systems. Taking radar signatures from a variety of azimuth and depression angles and combining them into a SAR image can provide accurate information about a building's layout. Moreover, information can be combined from a network of sensors, placed on different sides of the building, in order to enhance the imaging process. We modeled such a scenario in which two radars are placed on two orthogonal sides of the building, and the individual images obtained by each radar are added incoherently. The final (combined) SAR image enables us to clearly distinguish the interior and the back walls. The building layout and the SAR image obtained by Xpatch modeling are shown in Figures 13 and 14. The overall dimensions are 12.3 m x 7.5 m x 2.7 m, with 6" thick exterior walls (green) made of adobe (ε_r = 4.5-j0.4), drywall interior walls (yellow) including 2 x 4 wooden studs, glass windows (blue) and wooden doors (red). The radars operate at a center frequency of 2 GHz, with 2 GHz bandwidth, producing a down-range resolution of 7.5 cm. Each radar scans an aperture of 30^0 in azimuth, centered to the normal to the nearest wall. This example demonstrates how a network of STTW radars can be effectively employed together with SAR imaging in building mapping applications.

The next Xpatch modeling example considers a building interior that includes a number of weapon carrying people, dividing walls and metal furniture.

The building layout is shown in Fig. 15. The overall dimensions are 15.3 m x 11.4 m x 2.7 m. The exterior walls are 12" thick, the interior walls are 6" thick, and a floor is also included, all made of adobe (ε_r = 4.5-j0.1). The humans are equipped with AK47 rifles. Again, we model an ultra-wideband synthetic aperture radar, with an aperture of 42^0 in azimuth, centered at an oblique angle of 8^0 with respect to the front wall. The center frequency is 2 GHz, with 2 GHz bandwidth. The down-range resolution is 7.5 cm, whereas the cross-range resolution is 12.5 cm. The SAR image is shown in Fig. 16. The locations of the humans are indicated by small circles. Using an oblique look angle with respect to the front wall decreases the wall brightness in the image, therefore reducing the dynamic range necessary for detecting targets inside the room. However, the drawback of this technique is enhancing the multi-path propagation, which may result in "ghost images" showing up in the SAR images at wrong locations. One such location is indicated by a question mark in Fig. 16. We also notice that the metal furniture introduces strong clutter in the image, which, combined with multi-path propagation, may completely swamp the targets of interest. Another thing worth mentioning is that in all the examples above, the wall materials were in general uniform and presented moderate attenuation. Other construction techniques may involve walls with complicated structures, which introduce distortions in the imaging process, or highly attenuating (such as rebar concrete), which do not allow good electromagnetic wave penetration, even at relatively low frequencies.

4. CONCLUSIONS

The STTW technology is currently a critical component in the context of military operations in urban environment. While a number of STTW radar designs are already operational, most of them display relatively low resolution and are based on motion detection. The next generation of STTW radars will probably work as an array of sensors and will have high-resolution imaging capabilities, coupled eventually with change detection techniques. Our modeling efforts are focused in this direction, by providing the next generation radar designers with performance analysis, system parameter optimization, and understanding the limitations of their technical approaches.

In this paper we presented some of our work on modeling sensing through the wall radar scenarios. We employed electromagnetic modeling codes such as FDTD and Xpatch, and the hardware infrastructure available at the Army MSRC. One of our interests was in understanding the radar signature of the human body, and for this purpose we performed a detailed analysis by employing the FDTD simulation algorithm. We were also interested in larger scale simulations, on the size of large rooms or buildings, and we tackled these problems with Xpatch. Since Xpatch is an approximate solver, we were careful in validating this approach by comparing it with FDTD for typical scenarios. Throughout this work, the recurring theme was the ultra-wideband synthetic aperture radar technology, which enables operation at relatively low frequencies (for good wall penetration) and good resolution. The SAR images obtained in our simulations allowed us to draw encouraging conclusions regarding the feasibility and performance of such radar systems in STTW applications, although there are certain caveats and limitations that need to be taken into account.

REFERENCES

Andersh D., Hazlett M., Lee S.W., Reeves D., Sullivan D., and Chu Y, 1994: "Xpatch: A high-frequency electromagnetic scattering code and environment prediction for complex three-dimensional objects," *IEEE Antennas and Propagation Magazine*, Vol. 36, pp. 65-69, Feb. 1994.

Andersh D., Lee S. W., Moore J., Sullivan D., Hughes J., and Ling H., 1998: "Xpatch prediction improvements to support multiple ATR applications," *Proceedings of SPIE*, Vol. 3395, pp. 108-119, 1998.

Andersh D., Moore J., Kosanovich S., Kapp D., Bhalla R., Kipp R., Courtney T., Nolan A., German F., and Cook J., 2000: "Xpatch 4: The next generation in high- frequency electromagnetic modeling and simulation software," *The Record of the IEEE 2000 International Radar Conference*, pp. 844-849, May 2000.

Carin L., Geng N., McClure M., Sichina J. and Nguyen L., 1999: "Ultra-wide-band synthetic-aperture radar for mine-field detection," *IEEE Antennas and Propagation Magazine*, Vol. 41, pp. 18 – 33, Feb. 1999.

Lazzi G., Pattnaik S.S., Furse C.M., Gandhi O.P., 1998: "Comparison of FDTD computed and measured radiation patterns of commercial mobile telephones in presence of the human head," *IEEE Transactions on Antennas and Propagation*, Vol. 46, pp. 943-944, June 1998.

Ressler M.A. and McCorkle J.W., 1995: "Evolution of the Army Research Laboratory ultra-wideband test bed," in Ultra-Wideband Short-Pulse Electromagnetics 2, L. Carin and L.B. Felsen

eds., Plenum Press, NY, pp. 109-123, 1995.
Soumekh M., 1999: Synthetic Aperture Radar Signal Processing, John Wiley & Sons, 1999.
Taflove A., 1998: Advances in Computational Electrodynamics: The Finite-Difference Time-Domain Method, Artech, Norwood, MA, 1998.
Tinniswood A.D., Furse C.M., Gandhi O.P., 1998: "Computations of SAR distributions for two anatomically based models of the human head using CAD files of commercial telephones and the parallelized FDTD code," *IEEE Transactions on Antennas and Propagation*, Vol. 46, pp. 829-833, June 1998.
Toftgard J., Hornsleth S.N., Andersen J.B, 1993: "Effects of portable antennas in the presence of a person," *IEEE Transactions on Antennas and Propagation*, Vol. 41, pp. 739-746, June 1993.